

ORIGINAL ARTICLE

Insulin gene enhancer protein 1 mediates glycolysis and tumorigenesis of gastric cancer through regulating glucose transporter 4

Ting Guo^{1,†}  | Yan-Hua Bai^{2,†}  | Xiao-Jing Cheng¹  | Hai-Bo Han³  |
Hong Du¹  | Ying Hu³  | Shu-Qin Jia⁴  | Xiao-Fang Xing¹  | Jia-Fu Ji^{1,5} 

¹ Key Laboratory of Carcinogenesis and Translational Research (Ministry of Education/Beijing), Division of Gastrointestinal Cancer Translational Research Laboratory, Peking University Cancer Hospital & Institute, Beijing 100142, P. R. China

² Department of Pathology, Peking University Cancer Hospital & Institute, Beijing 100142, P. R. China

³ The Tissue Bank, Peking University Cancer Hospital & Institute, Beijing 100142, P. R. China

⁴ Department of Molecular Diagnosis, Peking University Cancer Hospital & Institute, Beijing 100142, P. R. China

⁵ Department of Gastrointestinal Surgery, Peking University Cancer Hospital & Institute, Beijing 100142, P. R. China

Correspondence

Jia-Fu Ji, Department of Gastrointestinal Surgery and Division of Gastrointestinal Cancer Translational Research Laboratory, Peking University Cancer Hospital & Institute, Beijing, 100142, P. R. China.

Email: jjiafu@hsc.pku.edu.cn

Xiao-Fang Xing, Key Laboratory of Carcinogenesis and Translational Research, Division of Gastrointestinal Cancer Translational Research Laboratory, Peking University Cancer Hospital & Institute, Beijing 100142, P. R. China.

Email: Xingxiaofang@bjmu.edu.cn

Shu-Qin Jia, Department of Molecular Diagnosis, Peking University Cancer Hospital & Institute, Beijing 100142, P. R. China.

Email: shuqin_jia@hsc.pku.edu.cn

†These authors contributed equally to this work.

Abstract

Background: Insulin gene enhancer protein 1, (ISL1), a LIM-homeodomain transcription factor, is involved in multiple tumors and is associated with insulin secretion and metabolic phenotypes. However, the role of ISL1 in stimulating glycolysis to promote tumorigenesis in gastric cancer (GC) is unclear. In this study, we aimed to characterize the expression pattern of ISL1 in GC patients and explore its molecular biological mechanism in glycolysis and tumorigenesis.

Methods: We analyzed the expression and clinical significance of ISL1 in GC using immunohistochemistry and real-time polymerase chain reaction (PCR). Flow cytometry and IncuCyte assays were used to measure cell proliferation after ISL1 knockdown. RNA-sequencing was performed to identify differentially expressed genes, followed by Kyoto Encyclopedia of Genes and Genomes (KEGG) analysis and Gene Set Enrichment Analysis (GSEA) to reveal key signaling pathways likely regulated by ISL1 in GC. Alteration of the glycolytic ability of GC cells with ISL1 knockdown was validated by measuring the extracellular acidification rate (ECAR) and oxygen consumption rate (OCR)

ABBREVIATIONS: 2-DG, 2-deoxy-D-glucose; ALDOA, Aldolase Fructose-Bisphosphate A; CDK4, cyclin-dependent kinases 4; CDK6, cyclin-dependent kinases 6; DEGs, differentially expressed genes; DFS, disease-free survival; ECAR, extracellular acidification rate; FCCP, p-trifluoromethoxy carbonyl cyanide phenylhydrazide; GC, Gastric cancer; GLUT1, glucose transporter type 1; GLUT4, Glucose transporter 4; GSEA, Gene set enrichment analysis; HDGF, hepatoma-derived growth factor; IGF1R, Insulin-Like Growth Factor Binding Protein 3; IgG, Immunoglobulin G; ISL1, Insulin gene enhancer protein 1; KEGG, Kyoto Encyclopedia of Genes and Genomes; LDHA, lactate dehydrogenase A; METTL3, methyltransferase like 3; OCR, oxygen consumption rate; OS, overall survival; PDK1, Pyruvate Dehydrogenase Kinase 1; PFKFB3, 6-phosphofructo-2-kinase/fructose-2,6-bisphosphatase 3; PKM2, Pyruvate Kinase M 2; p-Rb, phospho-retinoblastoma; SLC2A4, solute carrier family 2 member 4; STAT3, signal transducer and activator of transcription 3

This is an open access article under the terms of the [Creative Commons Attribution-NonCommercial-NoDerivs](https://creativecommons.org/licenses/by-nc-nd/4.0/) License, which permits use and distribution in any medium, provided the original work is properly cited, the use is non-commercial and no modifications or adaptations are made.

© 2021 The Authors. *Cancer Communications* published by John Wiley & Sons Australia, Ltd. on behalf of Sun Yat-sen University Cancer Center

Funding information

Natural Science Foundation of Beijing, Grant/Award Number: 7132051; National Natural Science Foundation of China, Grant/Award Numbers: 81301874, 81972758, 81872502, 81802471; Interdisciplinary Medicine Seed Fund of Peking University, Grant/Award Number: BMU2018MX018; Beijing Municipal Administration of Hospitals' Youth Program, Grant/Award Number: QML20181102; National High Technology Research and Development Program of China, Grant/Award Number: 2014AA020603; Science Foundation of Peking University Cancer Hospital, Grant/Award Numbers: 2017-23, 2020-6

and by detecting glucose consumption and lactate production. The expression of glucose transporter 4 (GLUT4) and ISL1 was assessed by Western blotting, immunohistochemistry, and immunofluorescent microscopy. The luciferase reporter activity and chromatin immunoprecipitation assays were performed to determine the transcriptional regulation of ISL1 on GLUT4.

Results: High levels of ISL1 and GLUT4 expression was associated with short survival of GC patients. ISL1 knockdown inhibited cell proliferation both *in vitro* and *in vivo*. KEGG analysis and GSEA for RNA-sequencing data indicated impairment of the glycolysis pathway in GC cells with ISL1 knockdown, which was validated by reduced glucose uptake and lactate production, decreased ECAR, and increased OCR. Mechanistic investigation indicated that ISL1 transcriptionally regulated GLUT4 through binding to its promoter.

Conclusion: ISL1 facilitates glycolysis and tumorigenesis in GC via the transcriptional regulation of GLUT4.

KEYWORDS

gastric cancer, glucose transporter 4, glycolysis, insulin gene enhancer protein 1, tumorigenesis

1 | BACKGROUND

Gastric cancer (GC), an aggressive malignancy with poor prognosis, is the fourth most common cancer in the world [1,2] and the second most common cancer in China [2]. Due to the lack of effective early diagnosis technology, most GC patients are diagnosed at advanced stages, and metastasis is the main cause of death in GC patients [3,4]. Revealing the mechanisms of carcinogenesis and metastasis of GC could lead to the identification of potential prognostic factors and potential therapeutic targets.

Insulin gene enhancer protein 1 (ISL1), a LIM-homeodomain transcription factor [5], regulates the expression of insulin, glucagon, somatostatin, and pancreatic polypeptide in postnatal islet tissue [6–8]. In addition to insulin gene regulation and glucose homeostasis, ISL1 affects cell fate specification and embryonic development [9–11]. It has been shown to induce metastasis and tumorigenesis in various cancers, including non-Hodgkin lymphoma [12], GC [13,14], pancreatic and extrapancreatic neuroendocrine neoplasms [15,16]. Generally, high ISL1 expression has been associated with poor outcomes of patients with GC [13,14]. However, the underlying molecular mechanism of ISL1 in promoting the glycolysis and tumorigenesis of GC remains to be elucidated. The “Warburg effect” in tumor cells promotes the glucose uptake, glycolysis, and pyruvate metabolism into lactic acid rather than oxidative phosphorylation to produce energy under aerobic conditions [17]. Compared with normal cells, tumor cells have shown stronger aerobic glycolysis and

higher glucose uptake [18]. Glycolytic genes and their transcriptional regulators are significantly associated with poor prognosis of various cancers, including GC, and the “Warburg effect” indicates the existence of a link between glycolysis and tumorigenesis [19–21]. As a result, cell metabolic disorders has been described as a hallmark of cancer that facilitates tumor progression [22]. Identifying the key factors which regulate glycolysis could therefore improve the diagnosis and treatment of GC.

Glucose transport across the cell membrane is a rate-limiting step in glycolysis, thus, glucose transporters play an important role in tumor initiation and progression [23,24]. Emerging evidence suggests that glucose transporter 4 (GLUT4), encoded by the solute carrier family 2 member 4 (SLC2A4) gene, is an attractive therapeutic target for cancer [25,26]. Furthermore, GLUT4 is insulin-sensitive and plays an essential role in glucose homeostasis [26]. Members of the GLUT family have tissue-specific expression, biochemical properties, and physiologic functions that operate together to regulate and maintain glucose levels and distribution. Recently, the expression of GLUTs was reported to modulate glucose metabolism and tumorigenesis in different cancers [27–30]. GLUT4 plays a central role in glucose metabolism and represents 90% of GLUTs [31].

Herein, this study aimed to explore the contribution of ISL1 and GLUT4 to the glycolysis and tumorigenesis of GC and to identify the underlying mechanisms. The significance of ISL1 and GLUT4 in the prognosis of GC patients was also analyzed.

2 | MATERIALS AND METHODS

2.1 | Cell culture

The GC cell line BGC823 was obtained from the Cell Research Institute (Shanghai, China), and HEK293FT cells were purchased from American type culture collection (ATCC, Manassas, VA, USA). The cells were cultured in high-glucose Dulbecco's modified eagle media (DMEM, Gibco, Grand Island, NY, USA) replenished with 10% (v/v) fetal calf serum (Gibco) and incubated in a humidified atmosphere containing 5% CO₂ at 37°C.

2.2 | Plasmids, short hairpin RNAs (shRNAs), and lentiviruses

The Flag-tagged GLUT4 in eukaryotic expression vector GV141 was purchased from Genechem (Shanghai, China). BGC823 cells were transfected with GLUT4 plasmids or control plasmids followed by 1 µg/mL purine (Gibco) screening for 2 weeks to obtain stable GLUT4-overexpressing or control cells. Lentiviral constructs pLenti6 were purchased from Invitrogen (Carlsbad, CA, USA). shRNA constructs were constructed by cloning shRNA fragments into pLenti-U6 (Invitrogen) and GV298 (Genechem). The sequences of shRNAs for ISL1 and GLUT4 knockdown are listed in [Supplementary Table S1](#).

Stable cell lines were established with a lentiviral vector using previously described protocols [32]. Briefly, lentiviruses were used to infect the cells for 2 days. Stable clones were selected by treating the cells with 3 µg/mL blasticidin (Gibco) for 2 weeks.

2.3 | Patients and gastric tissue specimens

Frozen GC tissues (stored at -70°C) were collected from 182 GC patients and paraffin-embedded GC tissues were collected from 167 GC patients who underwent radical resections before chemotherapy at the Peking University Cancer Hospital in 2010. The patients were followed up until 2019. This study was approved by the Ethics Committee of Peking University Cancer Hospital. All the patients provided written informed consent to allow the use of their data/tissues in research.

2.4 | Real-time PCR

To detect the mRNA levels of ISL1 and GLUT4, total RNA was extracted from the 182 frozen GC tissues using Trizol Reagent (Invitrogen) based on the manufacturer's instruc-

tions. Real-time PCR was performed using SYBR Green PCR Master Mix on ABI 7500 System (Applied Biosystems, Foster City, CA, USA) with different primers ([Supplementary Table S2](#)). All annealing temperatures were 60°C. Relative expression values for each gene were calculated using the $2^{-\Delta\Delta CT}$ method with normalization to Tubulin. Each value presents the average of at least 3 independent experiments.

2.5 | IHC of ISL1 and GLUT4 in tissue sections

The immunohistochemical (IHC) staining for ISL1 expression in 167 paraffin-embedded GC tissues and GLUT4 expression in 109 of the 167 GC tissues were evaluated independently by two experienced pathologists who were blinded to the patients' clinical outcomes. The discrepant cases were jointly reviewed to reach a consensus.

We randomly selected 42 GC tissues for IHC quantification of ISL1 and GLUT4 using TissueFAX cytometry (TissueGnostics, Vienna, Austria) according to the manufacturer's instructions. Images for ISL1 and GLUT4 staining were analyzed using HistoQuest software v3.5.3.0185 (TissueGnostics) [33,34]. The following parameters were adjusted: nuclei size, discrimination by area, discrimination by grey, and background threshold. The cells were counted with hematoxylin staining, and the positive rate of ISL1/GLUT4 was calculated with diaminobenzidine staining. We counted cells in GC tissues and peritumor tissues in the 42 samples (0.64 mm² area in each sample).

2.6 | Proliferation assays and flow cytometry

Stable GC cells were seeded in 96-well plates at a density of 3×10^3 cells/well, and cell confluence was detected with an IncuCyte Live-Cell imaging system (Essen BioScience, Ann Arbor, MI, USA). The cells were synchronized in the G₁ phase by incubation in a serum-free medium overnight and then with medium containing fetal bovine serum for 24 h. The samples were washed with phosphate buffer saline and stained with staining buffer for 15 min before flow cytometry (BD Biosciences, San Jose, CA, USA). All experiments were performed in triplicate, and three independent experiments were conducted.

2.7 | *In vivo* mouse models of GC cell lines

ISL1-knockdown and scramble BGC823 cells (3.5×10^5 cells per mouse) were subcutaneously injected into the right hind legs of 5-week-old female NOD/SCID mice

(Charles River, Beijing, China). This model was designed to detect subcutaneous tumorigenesis. ISL1-knockdown and scramble BGC823 cells (1.5×10^6 cells per mouse) were injected into the tail vein of female NOD/SCID mice. This model was designed to detect lung metastases. The lungs were removed at 3 weeks after inoculation and fixed with a picric acid fixative.

2.8 | Glycolysis assay

The glycolysis of BGC823 ISL1-knockdown, GLUT4-knockdown, and BGC823 scramble control cells was measured by examining glucose uptake and lactate secretion into the culture medium. The supernatants of these cells were harvested at 48 h after seeding and measured using a Glucose Uptake Colorimetric Assay Kit (Biovision, Milpitas, CA, USA) and a Lactate Colorimetric Assay Kit (Biovision) for glucose and lactate concentrations, respectively, according to the manufacturer's protocols.

2.9 | Extracellular acidification rate and oxygen consumption rate assays

The extracellular acidification rate (ECAR) and cellular oxygen consumption rate (OCR) were measured using Seahorse XF Glycolysis Stress Test Kit (Agilent Technologies, Palo Alto, CA, USA) and Seahorse XF Cell Mito Stress Test Kit (Agilent Technologies) and were analyzed using the Seahorse XF24 analyzer. Briefly, the glucose uptake of BGC823 ISL1-knockdown, GLUT4-knockdown, and scramble control cells were detected. These cells were harvested at 48 h after seeding, which were used to measure ECAR and OCR. After baseline measurements, for ECAR, the Seahorse automatically filled each well with 10 mmol/L glucose, 1 μ mol/L oligomycin (the oxidative phosphorylation inhibitor), and 50 mmol/L 2-DG (2-deoxy-D-glucose, the glycolytic inhibitor) successively. For OCR, 1 μ mol/L oligomycin, 1 μ mol/L FCCP (p-trifluoromethoxy carbonyl cyanide phenylhydrazine, the reversible inhibitor of oxidative phosphorylation), and 0.5 μ mol/L Rote/AA (rotenone plus the mitochondrial complex III inhibitor antimycin A, the mitochondrial complex I inhibitor) were automatically injected successively. Data were analyzed by using Seahorse XF24 Wave software. ECAR in mpH/min and OCR in pmol/min are reported. The following reagents were all obtained from Agilent Technologies: XF DMEM Base Me (103575-100), XF 200 mmol/L Glutamine Solution (103579-100); Seahorse XFe24 Fluxpak mini (102342-100); XF 1.0 mol/L Glucose Solution (102342-100); XF 100 mmol/L Pyruvate (103578-100); Seahorse XF Glycolysis Stress Test Kit (103020-100); Seahorse XF Cell Mito Stress Test Kit (103015-100).

2.10 | Immunofluorescence

Immunofluorescence was implemented as previously reported [13]. Briefly, BGC823 ISL1-knockdown, GLUT4-knockdown, and scramble cells were fixed in 4% paraformaldehyde for 20 min, cultured in blocking buffer, then incubated with primary antibodies against GLUT4 and ISL1, followed by incubation with Alexa Flour donkey anti-rabbit and donkey anti-mouse antibodies (Invitrogen). The 4',6-diamidino-2-phenylindole 4 (DAPI, Invitrogen) binding to DNA can be used to observe nuclear condensation [35]. The images were obtained by laser scanning confocal microscope LSM 780 with Zen software under a 63 \times oil-immersed lens (Carl Zeiss, Toronto, ON, Canada). The details of the antibodies used are listed in [Supplementary Table S3](#).

2.11 | Luciferase reporter assay

The human GLUT4 gene promoter region (2000 bp) was inserted into the pGL₃ basic vector (Promega, Madison, WI, USA) to construct the pGL₃-GLUT4 promoter. Then, 100 ng of the constructed plasmid and 7 ng Renilla luciferase control plasmid (Promega) were transfected into BGC823 cells in 24-well plates. After 48 h, luciferase activities were determined using a Dual-Luciferase Assay kit (Promega).

2.12 | Chromatin immunoprecipitation (ChIP) assay

ChIP was performed as previously described [36]. In brief, the cross-linked and isolated nuclei were ultrasonically treated with a Diagenode Bioruptor (Sonics & Materials, Newtown, CT, USA) to an average size of \sim 500 bp for ChIP-qPCR. The annealing temperature was 60°C. After pre-clearing with bovine serum albumin (BSA)-blocked protein A/G Sepharose (Roche, Mannheim, Germany), chromatin was incubated with antibodies at 4°C overnight. The chromatin immune complexes were recovered with the same BSA-blocked protein A/G beads. The sequences of primers are provided in [Supplementary Table 2](#).

2.13 | RNA sequencing and data analysis

RNA sequencing was performed to confirm the stable knockdown of ISL1. Gene expression levels were calculated using fragments per kilobase of transcript per million mapped reads, and the data were deposited in the Gene Expression Omnibus (GEO, <https://www.ncbi.nlm.nih.gov/geo/query/acc.cgi?acc=GSE147006>). Kyoto

encyclopedia of genes and genomes (KEGG) analysis and Gene Ontology (GO) enrichment analysis of differentially expressed genes (DEGs) were performed using the cluster Profiler R package [37]. Significant GO terms were identified with $P < 0.05$. Pathway analysis based on the differentially expressed genes between ISL1 knockdown and the scramble control was performed using gene set enrichment analysis (GSEA) JAVA program (<http://software.broadinstitute.org/gsea/index.jsp>) [38]. The analysis was conducted with 1000 gene set permutations, and pathways were ranked based on their enrichment scores; the top 20 pathways were selected for further validation.

2.14 | Statistical analysis

The overall survival (OS) was calculated from the date of surgery till the death due to any reason. The disease-free survival (DFS) was calculated from the date of surgery till the occurrence of any complications during follow-up. The survival data of GC cases in 5 GC datasets (GSE14210, GSE15459, GSE22377, GSE29272, and GSE51105) covering a total of 876 patients were graphically presented by Kaplan-Meier plotter (<http://kmplot.com/analysis/>) [39] and analyzed using log-rank test. The correlation between ISL1 expression and GLUT4 expression in the 182 primary GC specimens, the 42 selected paraffin-embedded GC tissues, and the public GC dataset from The Cancer Genome Atlas (TCGA, obtained from the Gene Expression Profiling Interactive Analysis, GEPIA, <http://gepia.cancer-pku.cn/>) [40] was analyzed by using Pearson's correlation coefficient (r).

The continuous data are expressed as the mean \pm standard deviation. Comparisons between groups were analyzed using the Student's t -test or Analysis of Variance by SPSS 22.0 statistical software (IBM SPSS, Armonk, NY, USA), and the Student-Newman-Kleuss method was used to estimate the level of significance. Differences were considered statistically significant at two-side $P < 0.05$.

3 | RESULTS

3.1 | High ISL1 expression predicts poor outcomes in patients with GC

The expression of ISL1 in 167 paraffin-embedded GC specimens was investigated by IHC. ISL1 protein expression was quantified in 42 samples covering 140,420 cells in GC tissues and 52,327 cells in peritumor tissues using the Tissue-FAX cytometry. The mean positive rate of ISL1 in GC cells was 57.9% (Figure 1A and B).

Next, we investigated the ISL1 expression in 182 frozen paired primary GC tissues and adjacent normal tissues using real-time PCR and observed that ISL1 was highly expressed in GC tissues (Figure 1C). We divided patients into high and low ISL1 expression groups using the X-tile program [41] (Supplementary Figure S1A and B). The patients with high ISL1 expression had shorter OS ($P < 0.001$) and DFS ($P < 0.001$) than those with low ISL1 expression (Figure 1D). The same results were observed between the ISL1-positive and -negative groups (Supplementary Figure S1C) and in the 5 GC datasets ($P = 0.004$, Supplementary Figure S1D). These results suggested that high ISL1 expression could be a biomarker of poor prognosis in patients with GC.

3.2 | ISL1 knockdown inhibits GC cell tumorigenesis *in vitro* and *in vivo*

BGC823 cells were stably transfected with specific shRNA to knockdown ISL1; cells transfected with scramble shRNA were used as control (Figure 2A). ISL1 knockdown inhibited the proliferation of BGC823 cells by 38% at 72 h, as observed using IncuCyte assay (Figure 2B).

To further confirm the impact of ISL1 on the proliferation of GC cells, the cell cycle profile was analyzed using propidium iodide staining and flow cytometry. Compared with the scramble control, ISL1 knockdown was associated with increased cell population in the G₁ phase and decreased cell population in the G₂/M and S phases (Figure 2C and D). Consistently, the levels of phospho-retinoblastoma (p-Rb), P21, and P27 were increased, whereas those of Cyclin-dependent kinases 4 (CDK4), Cyclin-dependent kinases 6 (CDK6), Cyclin D1, and Cyclin D3 were decreased in response to ISL1 knockdown (Figure 2E). These data indicated that ISL1 knockdown impaired GC cell proliferation.

To further demonstrate the tumorigenic ability of ISL1 on GC *in vivo*, xenograft tumor models were established by subcutaneous injection of BGC823 cells with or without ISL1 knockdown. Compared with the scramble control group, the ISL1 knockdown group had a smaller tumor size and slower tumor growth rate (Figure 2F). To examine the effects of ISL1 on tumor metastatic colonization, ISL1-knockdown or scramble control BGC823 cells were injected into NOD/SCID mice via the tail vein. Metastatic potential was assessed by counting the colonized tumor nodules in the lungs. Fewer lung tumor nodules were observed in the ISL1 knockdown group than in the scramble control group (Figure 2G). Taken together, these data indicate that ISL1 knockdown significantly inhibited tumorigenesis of BGC823 cells.

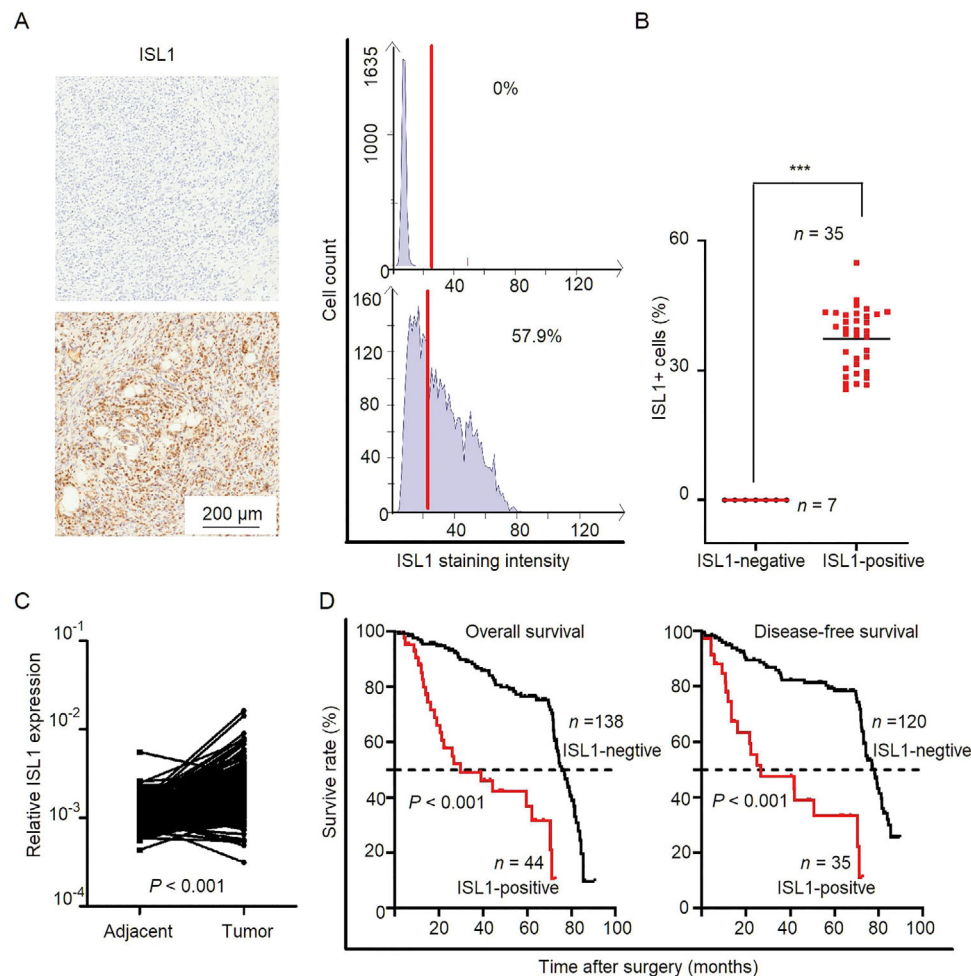


FIGURE 1 High ISL1 expression is a marker for poor prognosis during GC progression. A and B: TissueFAX cytometric quantification of ISL1 protein expression. A: Representative images and histograms of ISL1 staining. The upper image demonstrates negative ISL1 staining, and the lower image demonstrates positive ISL1 staining. The red line indicates the average intensity of 57.9%. B: Scatter plot of ISL1 staining by TissueFAX cytometric quantification. Of the 42 GC samples, 7 were ISL1-negative, and 35 were ISL1-positive. C: The mRNA expression of ISL1 in 182 paired GC and adjacent normal tissues was analyzed by real-time PCR with Tubulin as the reference gene. D: Kaplan-Meier OS and DFS curves demonstrate poor prognosis in patients with high ISL1 expression *versus* those with low ISL1 expression in GC tissues. Abbreviations: ISL1: insulin gene enhancer protein 1; GC: gastric cancer; OS: overall survival; DFS: disease-free survival; PCR: polymerase chain reaction; *n*: number

3.3 | ISL1 regulates glycolytic gene expression

To confirm ISL1 downstream effectors, we implemented RNA-sequencing through stable ISL1-knockdown or scramble control cells. The results displayed a total of 1112 ISL1-responsive genes, of which 582 were up-regulated (fold change > 2, $P < 0.01$) and 584 were down-regulated (fold change < 0.1, $P < 0.01$, Figure 3A, Supplementary Figure S2). KEGG analysis showed that the glycolysis pathway was among the most altered pathways upon ISL1 knockdown. Subsequent pathway analysis showed that several of the pathways altered after ISL1 knockdown were related to the regulation of glucose transport (a prerequisite process for tumor invasion) and glycolysis

(Figure 3B). Several glycolysis-related genes, including GLUT4, GLUT1, lactate dehydrogenase A (LDHA), and 6-phosphofructo-2-kinase/fructose-2,6-biphosphatase 3 (PFKFB3), were significantly down-regulated upon ISL1 silencing, among which the expression of GLUT4 was the most attenuated (Figure 3C). GSEA showed the enrichment of pathways involving glycolysis/gluconeogenesis (Figure 3D) and glycosphingolipid biosynthesis (Supplementary Figure S3). Together with the results of KEGG analysis (Figure 3B), glycolysis was identified as the key pathway affected by ISL1 knockdown. Other pathways related to tumor progression, such as the epithelial-to-mesenchymal transition, G₂M checkpoint, apoptosis, P53, and signal transducer and activator of transcription 3 (STAT3) pathways, were also enriched in GSEA

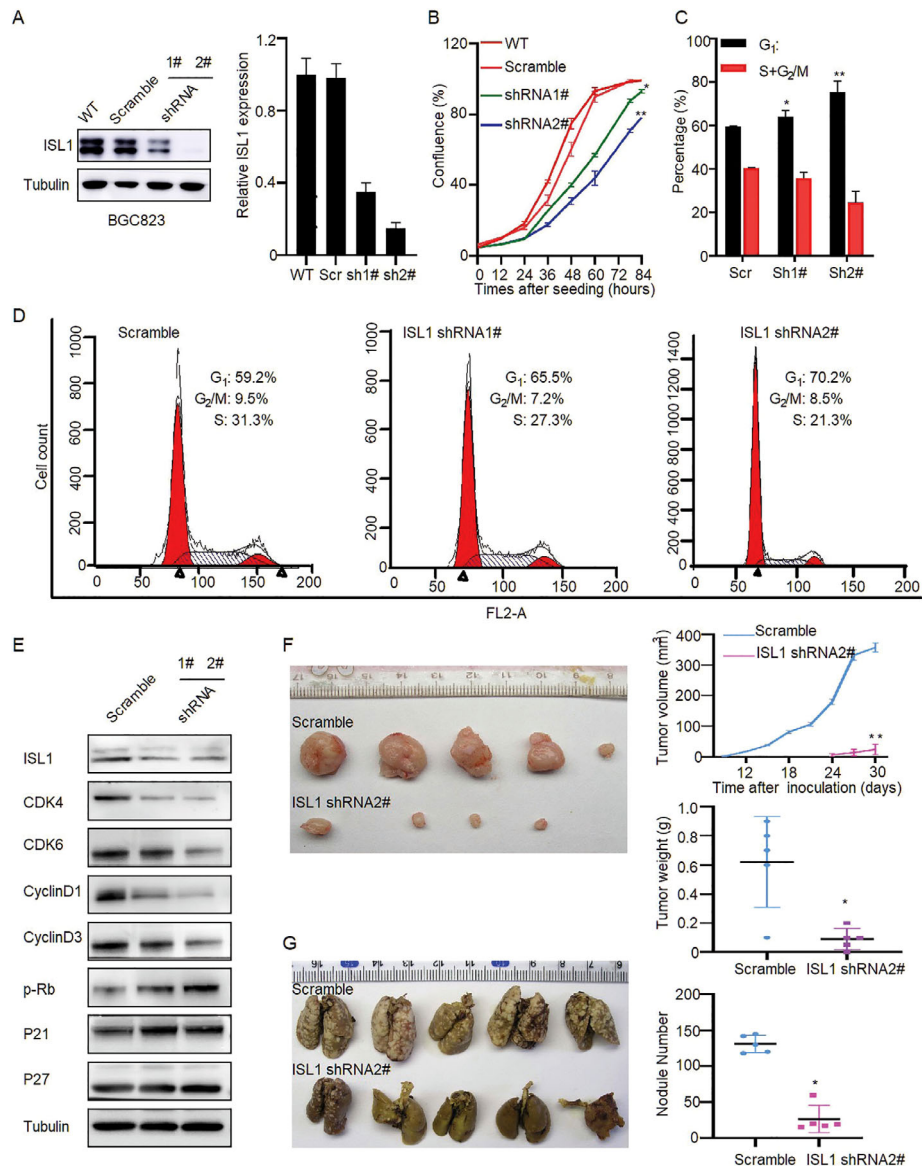


FIGURE 2 ISL1 knockdown inhibits GC cell tumorigenesis *in vitro* and *in vivo*. A: Stable down-regulation of ISL1 expression in BGC823 cells after ISL1 knockdown was confirmed by Western blotting and real-time PCR. B: Stable cell proliferation was monitored with an IncuCyte system every 6 h after seeding. C, D: GC cell cycle analysis by flow cytometry. E: Western blotting for the cell cycle-related proteins in BGC823 cells with stable ISL1 knockdown and scramble control. F: Photographs of tumors formed in mice injected with ISL1-knockdown or scramble control BGC823 cells. G: The influence of blood circulation on lung metastasis. Each bar in panels A–C represents the mean \pm SD from 3 independent experiments. * $P < 0.05$, ** $P < 0.01$. Abbreviations: ISL1: insulin gene enhancer protein 1; GC: gastric cancer; WT: wild-type; Scr: scramble control; sh1#: shRNA1#; sh2#: shRNA2#; PCR: polymerase chain reaction; p-Rb: phospho-retinoblastoma; CDK4: Cyclin-dependent kinase 4; CDK6: Cyclin-dependent kinase 6; SD: standard deviation

(Supplementary Figure S3), which is consistent with the results of previous studies [6,11,13,14]. Since ISL1 was implicated in the regulation of glycolytic gene expression, we next tested whether it modulates the glycolytic phenotype in cultured cells. ISL1 knockdown decreased glucose uptake, lactate production (Figure 3E), and ECAR (Figure 3F) and increased OCR in BGC823 cells (Figure 3G), indicating compromised aerobic glycolysis and improved aerobic oxidation.

3.4 | GLUT4 is a transcriptional target of ISL1

Since GLUT4 expression was attenuated the most by ISL1 knockdown and it plays a pivotal role in glycolysis to promote cancer progression [30,42], we next focused on the role of ISL1 on GLUT4 expression. Immunofluorescence analysis showed that knockdown of ISL1 significantly reduced GLUT4 expression on the cell membrane

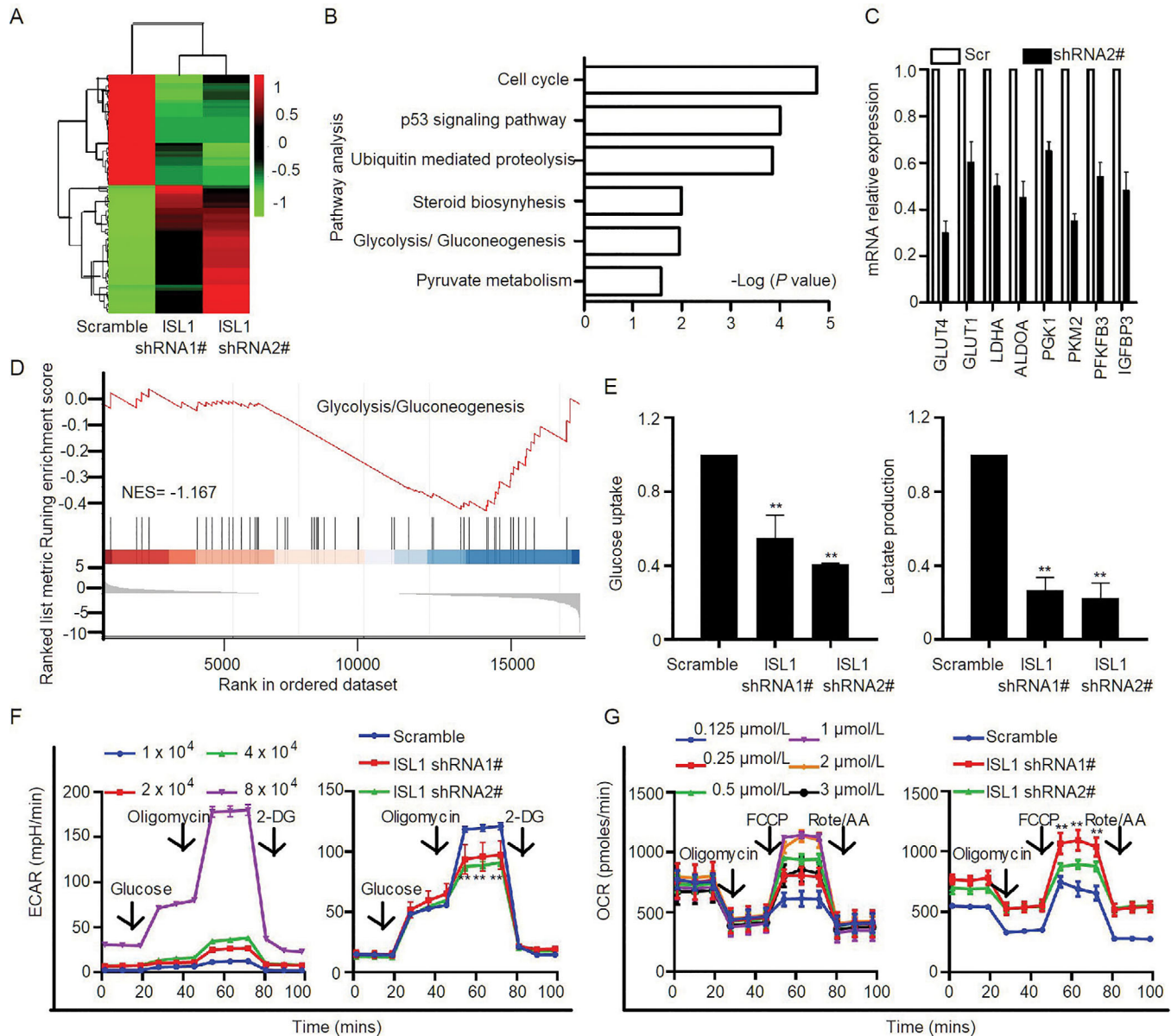


FIGURE 3 ISL1 regulates glycolytic gene expression. A: Heatmap of RNA-sequencing in BGC823 cells transfected with ISL1-shRNA1#, ISL1-shRNA2#, or scramble shRNA. Red color indicates up-regulated genes, and green color indicates down-regulated genes. B: KEGG analyses of DEGs in BGC823 cells upon ISL1 knockdown. C: Real-time PCR validation of DEGs that were related to glycolysis. D: Gene set enrichment analysis (GSEA) for gene signatures of glycolysis in BGC823 cells with stable ISL1 knockdown. E: Glucose uptake and lactate secretion by BGC823 cells with stable ISL1 knockdown. F: ECAR of stable ISL1-knockdown or scramble control BGC823 cells were measured at 1×10^4 , 2×10^4 , 4×10^4 , and 8×10^4 cells/well, and 4×10^4 cells/well is the appropriate cell gradient. The Seahorse automatically filled each well with 10 mmol/L glucose, 1 μ mol/L oligomycin, and 50 mmol/L 2-DG successively. G: OCR of stable ISL1-knockdown or scramble control BGC823 cells treated with 0.125, 0.25, 0.5, 1, 2, and 3 μ mol/L FCCP were measured, and 1 μ mol/L was the appropriate concentration. For OCR, 1 μ mol/L oligomycin, 1 μ mol/L FCCP, and 0.5 μ mol/L Rote/AA were automatically injected successively. Each bar represents the mean \pm SD of three independent experiments. * $P < 0.05$, ** $P < 0.01$, vs. the scramble control. Abbreviations: ISL1: insulin gene enhancer protein 1; KEGG: Kyoto Encyclopedia of Genes and Genomes; DEGs: differentially expressed genes; PCR: polymerase chain reaction; GSEA: gene set enrichment analysis; ECAR: extracellular acidification rate; OCR: oxygen consumption rate; 2-DG: 2-deoxy-D-glucose; FCCP: the reversible inhibitor of oxidative phosphorylation; Rote/AA: rotenone plus the mitochondrial complex III inhibitor antimycin A; GLUT4: Glucose transporter 4; GLUT1: glucose transporter type 1; LDHA: lactate dehydrogenase A; ALDOA: aldolase fructose-bisphosphate A; PKM2: pyruvate kinase M 2; PDK1: pyruvate dehydrogenase kinase 1; IGF1BP3: insulin-like growth factor binding protein 3; PFKFB3: 6-phosphofructo-2-kinase/fructose-2,6-bisphosphatase 3; SD: standard deviation

(Figure 4A). The expression patterns of ISL1 and GLUT4 were similar in GC tissues. High ISL1 expression was often accompanied by high GLUT4 expression, and GLUT4 generally showed low expression when ISL1 was expressed at low levels (Figure 4B). Consistent with these observations, GLUT4 was down-regulated by ISL1 silencing at both the mRNA and protein levels (Figure 4C).

To further characterize the regulation of ISL1 on GLUT4 transcription, we performed ChIP and luciferase reporter activity assays. The ChIP assay revealed a 15-fold ISL1 enrichment on the GLUT4 promoter in BGC823 cells (Figure 4D), suggesting that ISL1 could bind to the GLUT4 promoter to regulate GLUT4 transcription. Furthermore, luciferase reporter activity assays showed that ISL1 overexpression could activate the wild-type GLUT4 reporter but failed to activate the mutant GLUT4 reporter at the predicted ISL1-binding site (Figure 4E), indicating that ISL1 directly regulated the transcription of GLUT4 by binding to its promoter.

3.5 | GLUT4 mediates the promotion of aerobic glycolysis by ISL1 in GC cells

We next examined whether GLUT4 mediated the promoting effect of ISL1 on glycolysis in BGC823 cells. We constructed stable cell lines with efficient knockdown of GLUT4 (Figure 5A) and overexpression of GLUT4 (Figure 5B). Successful overexpression of GLUT4 reversed the effects of ISL1 knockdown on glucose consumption, lactate production, ECAR, and cellular OCR (Figure 5C and D compared with Figure 3E–G). With efficient knockdown of GLUT4, glucose consumption, lactate production, and ECAR were significantly decreased while the cellular OCR was increased (Figure 5E and F), suggesting the necessity of GLUT4 in maintaining glucose metabolic reprogramming in GC cells, as previously reported [30,43].

3.6 | GLUT4 predicts poor outcomes in patients with GC

Finally, we investigated the clinical significance of GLUT4 expression in 109 primary GC specimens using IHC. GLUT4 protein expression was quantified in 42 samples covering 118,706 cells in GC tissues and 34,466 cells in peritumor tissues by using the TissueFAX cytometry. The mean positive rate of GLUT4 in GC cells was 25.9% (Figure 6A and B). GLUT4 and ISL1 expression in the 42 GC specimens was positively correlated ($r = 0.41$, $P = 0.008$; Figure 6C). The correlation of ISL1 and GLUT4 expression was also confirmed using the public GC dataset from TCGA ($r = 0.62$, $P < 0.001$; Figure 6D). Kaplan-Meier sur-

vival curves showed that patients with positive GLUT4 staining had a significantly shorter OS than those with negative GLUT4 staining ($P = 0.007$; Figure 6E). The association between GLUT4 expression and OS was confirmed using data from the Kaplan-Meier plotter ($P < 0.001$; Figure 6F). Next, we investigated GLUT4 expression in 182 paired primary GC tissues and adjacent normal tissues using real-time PCR. GLUT4 was highly expressed in GC tissues and positively correlated with ISL1 expression ($r = 0.43$, $P < 0.001$; Figure 6G). In addition, X-tile analysis indicated that high GLUT4 expression predicted short survival in patients with GC ($P < 0.001$; Figure 6H, Supplementary Figure S4). Collectively, these results suggest that GLUT4 predicts poor outcomes in patients with GC and that ISL1 influences glycolysis through GLUT4.

4 | DISCUSSION

ISL1 had long been known as an important regulator of glucose homeostasis through modulation of insulin gene expression in pancreatic cells, this study demonstrated direct regulation of ISL1 on glucose metabolism in cancer cells.

Aberrant gene expression or enzymatic activity accounting for glucose uptake and the three committed steps of glycolysis represent general mechanisms for glucose metabolism reprogramming in cancer cells. Oncogenic drivers and tumor suppressors are able to affect glucose metabolism through multiple mechanisms. Hypoxia-inducible factor 1 (HIF1) had been shown to up-regulate the expression of GLUT1 and hexokinase 2 (HK2) to increase glucose uptake and phosphorylation [44,45]; oncogenic KRAS (KRAS proto-oncogene, GTPase) and BRAF (B-Raf proto-oncogene, serine/threonine kinase) not only increased the expression of GLUT1 but also promoted its translocation to the plasma membrane [46]. Transcriptional targets of c-Myc during glycolysis include HK2, LDHA, and monocarboxylate transporter (MCT) [47]. According to the results of RNA sequencing in the present study, besides GLUT4 knockdown, ISL1 knockdown also resulted in down-regulation of GLUT1, LDHA, and PFKFB3, which contributed to augmented glycolysis in cancer cells [48]. ISL1 may affect glycolysis-related genes in GC cells, comparable to those well-known oncoproteins mentioned above. Intriguingly, we previously showed that ISL1 was able to promote c-myc transcription and pancreatic islet cell proliferation [49]. The coordination between ISL1 and other oncoproteins like c-myc in glycolysis regulation in GC merits further investigation.

Glycolysis is a core pathway of cell carbon metabolism, which provides energy in the form of ATP and fuels cell growth and division [26]. High glycolysis flux was not

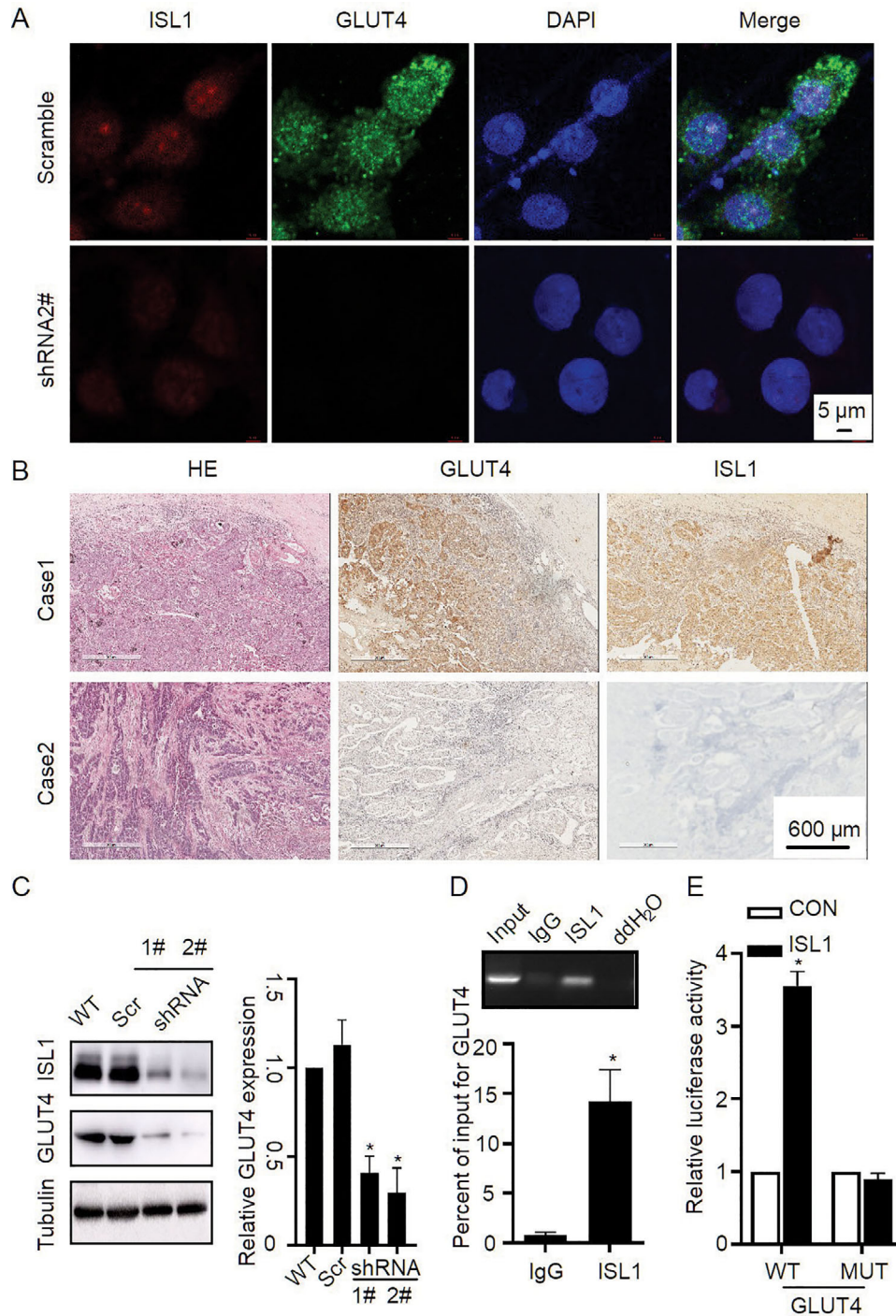


FIGURE 4 GLUT4 is a transcriptional target of ISL1. A: Effect of ISL1 knockdown on GLUT4 expression and subcellular distribution. B: Expression patterns of ISL1 and GLUT4 in GC tissues. ISL1 and GLUT4 show consistent expression patterns in GC tissues. High ISL1 expression is often accompanied by high GLUT4 expression (case 1), and GLUT4 is always expressed at low levels when ISL1 is expressed at low levels (case 2). C: Western blotting analysis of the effect of ISL1 silencing on GLUT4 expression at both transcriptional and protein levels in BGC823 cells. D: ChIP analysis of the ISL1 recruitment onto the GLUT4 promoter. The resulting input and ChIP DNA were characterized with PCR primers specific for GLUT4 genomic loci to calculate the percentage of coprecipitated DNA relative to the input. E: Luciferase reporter assay was performed in 293FT cells. Abbreviations: GLUT4: glucose transporter 4; ISL1: insulin gene enhancer protein 1; GC: gastric cancer; DAPI: 4',6-diamidino-2-phenylindole 4; HE: hematoxylin-eosin; ChIP: chromatin immunoprecipitation assay; IgG: immunoglobulin G; PCR: polymerase chain reaction; CON: control; MUT: mutant

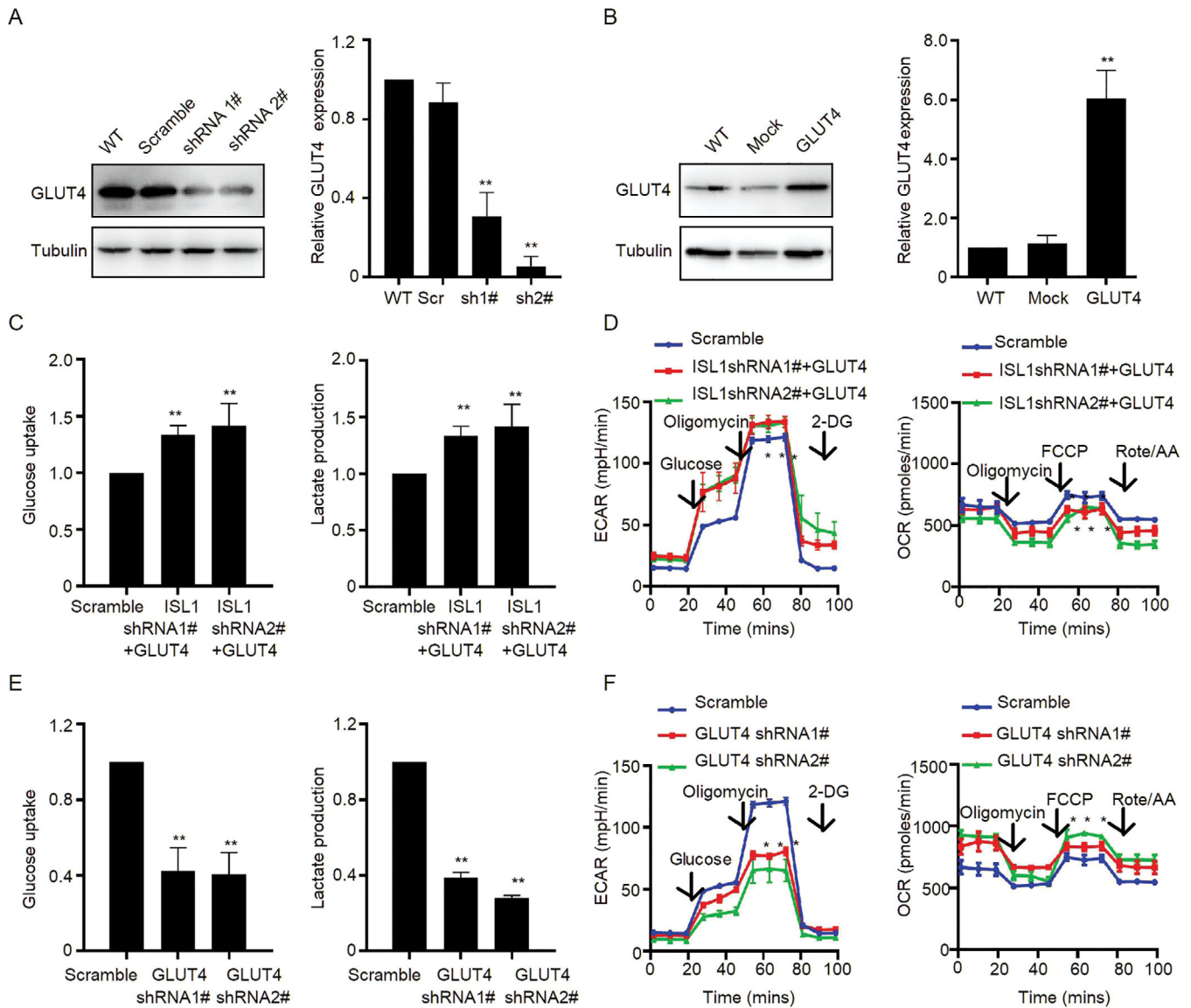


FIGURE 5 GLUT4 mediates the effect of ISL1 on glycolysis in GC. A: The effect of GLUT4 knockdown in BGC823 cells was determined by real-time PCR and Western blotting. B: The effect of GLUT4 overexpression in ISL1-knockdown BGC823 cells was determined by real-time PCR and Western blotting. C and D: Effect of GLUT4 overexpression on glucose consumption, lactate production (C), and ECAR or cellular OCR (D) in ISL1-knockdown BGC823 cells. E and F: Effects of GLUT4 knockdown on glucose consumption, lactate production (E), and ECAR or cellular OCR (F) in BGC823 cells. Abbreviations: GLUT4: glucose transporter 4; ISL1: insulin gene enhancer protein 1; GC: gastric cancer; WT: wild-type; Scr: scramble control; sh1#: shRNA1#; sh2#: shRNA2#; PCR: polymerase chain reaction; ECAR: extracellular acidification rate; OCR: oxygen consumption rate

simply an accompanying phenomenon but was supposed to confer selective advantages to cancer cells from several perspectives, including rapid ATP synthesis, biogenesis of macromolecules, and disruption of tissue integrity [17]. Thus, cancer cell proliferation, metastasis, and glycolysis are functionally intertwined during tumor progression. Consistently, the present study showed that ISL1 promoted GC growth *in vitro* and *in vivo*, accompanied by the regulation of gene expression involved in cell cycle, P53 signaling, and some other pathways. Any alteration

or mutation within the DNA-binding domain of P53 may lead to the dysregulation or overexpression of GLUT4 in certain types of cancer [50]. Meanwhile, we have also previously shown that ISL1 regulated ZEB1 (zinc finger E-box binding homeobox 1) expression and metastasis in GC [13]. The regulatory hierarchy of ISL1 on glucose metabolism reprogramming, cell cycle progression, and metastasis in GC merits further investigation.

Mediating the entry of glucose into cells, GLUTs have always been considered to be potential targets for

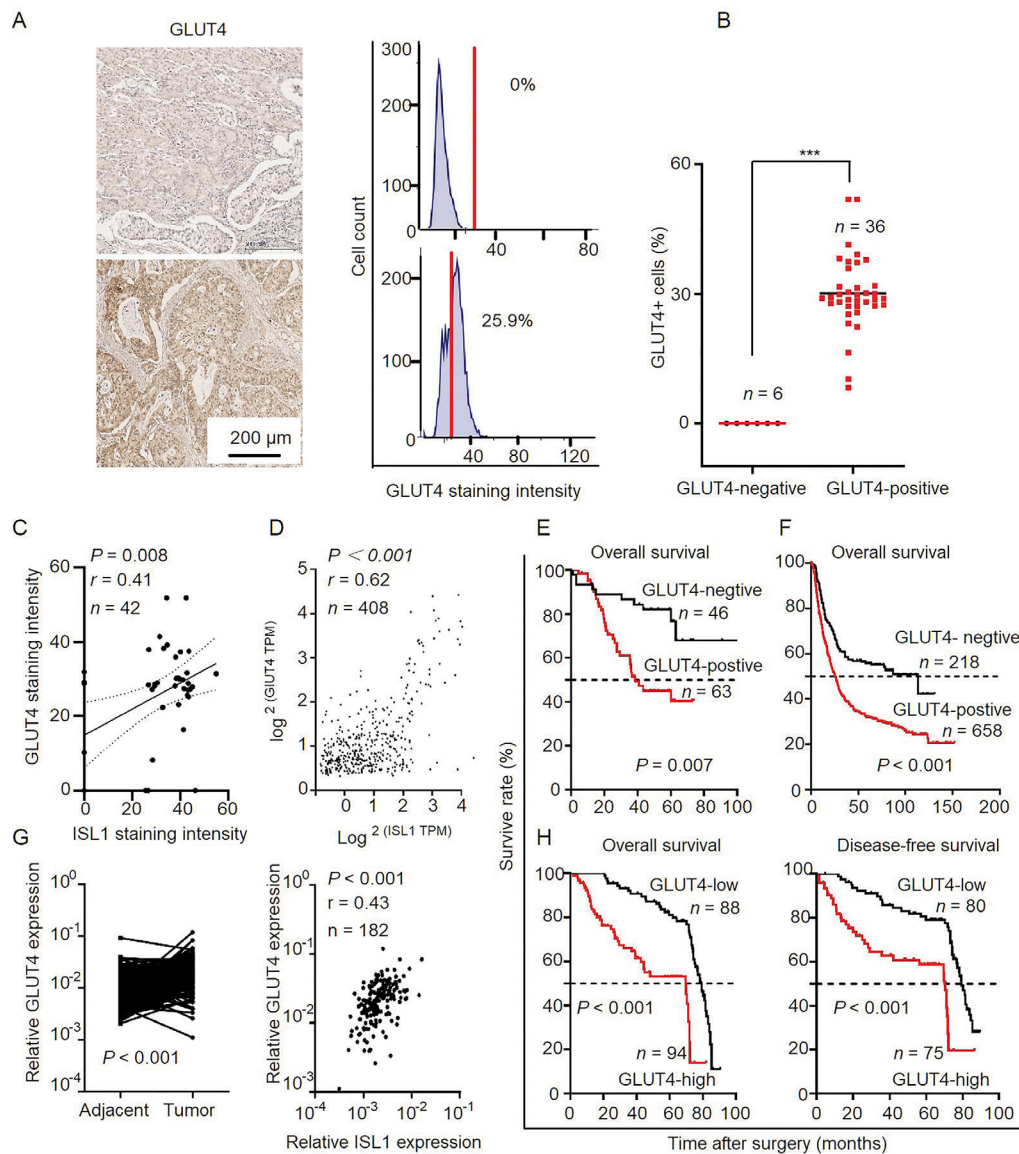


FIGURE 6 GLUT4 predicts poor outcomes in patients with GC. A-B: TissueFAX cytometric quantification of GLUT4 protein expression. A: Representative images and histograms of GLUT4 staining. The upper panel is the negative representative picture, and the lower panel is the positive representative picture, events represent the cells count; intensity represents the intensity of GLUT4 staining. The red line indicates that the average intensity is 25.9%. B: Scatter plot of GLUT4 staining by TissueFAX cytometric quantification. Six of the 42 samples were GLUT4 negative staining and thirty-six were GLUT4 positive staining. C: The correlation between GLUT4 and ISL1 expression was observed in the protein analysis by the TissueFAX cytometry. D: GEPIA results indicate a correlation between ISL1 and GLUT4 gene expression in stomach adenocarcinoma samples from the TCGA. E: Kaplan-Meier survival curves of survival time for patients with positive versus negative GLUT4 expression. F: Kaplan-Meier survival analysis of overall survival. The data were obtained from publicly available gene expression datasets. G: The mRNA expression of GLUT4 was analyzed by real-time PCR in 182-paired GC samples with Tubulin as the reference gene. H: Kaplan-Meier curves of OS and DFS for patients showed poor prognosis in high GLUT4 expression *versus* low GLUT4 expression in GC tissues. Abbreviations: GLUT4: glucose transporter 4; ISL1: insulin gene enhancer protein 1; GC: gastric cancer; GEPIA: the Gene Expression Profiling Interactive Analysis; TPM: transcripts per million; TCGA: The Cancer Genome Atlas; PCR: polymerase chain reaction; OS: overall survival; DFS: disease-free survival

cancer treatment. Elucidating the regulatory mechanism of GLUTs could be helpful to make therapeutic choice. For example, small molecules (STF-31 and STF-66247) inhibiting GLUT1 were supposed to treat oncogenic KRAS- or

BRAF-positive cancers and have been shown to selectively kill renal cell carcinoma cells [51]. Inhibition of GLUT4 was shown to elicit growth arrest and cell apoptosis in multiple myeloma [25]. In GC, GLUT4 was recently shown to

be regulated by hepatoma-derived growth factor (HDGF) in a methyltransferase-like 3 (METTL3)-dependent manner [52] and by Krüppel-like transcription factor 8 (KLF8)[30], and contributed to the oncogenic functions of METTL3 and KLF8. Together with our discovery, it is quite interesting to explore the functional relevance among ISL1, METTL3, and KLF8 during GC development. Moreover, the efficacy of GLUT4 inhibitors on ISL1-, METTL3-, and KLF8-positive GC is worth further investigation.

Regulation of gene expression by ISL1 generally involves its interaction with other epigenetic enzymes/complexes [53,54]. We also demonstrated that ISL1 recruited set domain-containing 7/9 (SET7/9) and jumonji domain-containing protein 3 (JMJD3) to maintain insulin gene expression under normal glucose [8]. SET7/9 also facilitated ISL1-mediated ZEB1 transcription in GC cells through methylation of histone 3 lysine 4 (H3K4) [13]. Epi-enzymatic cofactors for ISL1 at the loci of GLUT4 or other potential targets during glycolysis regulation are currently unknown. Promoter (enhancer)-based DNA pull-down assays may help discover epi-enzymatic cofactors for ISL1. Meanwhile, altered glucose metabolism is not merely byproduct of the oncogenic drivers but also participates in the epigenetic reprogramming of chromatin through altered intermediate metabolites that usually function as substrates or cofactors for certain epigenetic enzymes [55].

As ISL1 was recently identified as a pioneer factor and shaped the chromatin landscape of cells during certain biological processes [53], another emerging question is whether GLUT4-mediated glycolysis contributes to ISL1-mediated chromatin remodeling and dysregulated gene expression during GC development, which needs further investigation.

5 | CONCLUSIONS

This study revealed that ISL1 modulates tumorigenesis and glycolysis in GC and that silencing ISL1 expression impairs glycolysis through regulating GLUT4 in GC cells. Moreover, ISL1 and GLUT4 are predictive markers of poor prognosis in patients with GC, which might hold therapeutic potential for this lethal malignancy.

ACKNOWLEDGEMENTS

We sincerely appreciate the generous help from Dr. Bin Dong and Dr. Xi-Juan Liu in the Department of Core Laboratory at the Peking University Cancer Hospital for excellent assistance in evaluating the immunohistochemistry results and flow cytometry experiments. We would like to thank Editage (www.editage.cn) for English language editing.

ETHICS APPROVAL AND CONSENT TO PARTICIPATE

All the patients provided written informed consent to allow the use of their data/tissues in research. All procedures performed in this study involving animal experiments were in accordance with the National Institutes of Health guide for the care and use of laboratory animals and approved by the Animal Care and Use Committee of Peking University Cancer Hospital (2013KT25).

CONSENT FOR PUBLICATION

Not applicable.

COMPETING INTERESTS

The authors declare that they have no competing interests

AVAILABILITY OF DATA AND MATERIAL

The RNA sequencing data were deposited in the Gene Expression Omnibus (GEO, <https://www.ncbi.nlm.nih.gov/geo/query/acc.cgi?acc=GSE147006>), Kaplan-Meier plotter (<http://kmplot.com/analysis/>), and GEPIA (<http://gepia.cancer-pku.cn/>).

FUNDING

This work was supported by the Natural Science Foundation of Beijing (No. 7132051), the National Natural Science Foundation of China (Nos. 81301874, 81972758, 81872502, 81802471), the Interdisciplinary Medicine Seed Fund of Peking University (No. BMU2018MX018), Beijing Municipal Administration of Hospitals' Youth Program (No. QML20181102), the National High Technology Research and Development Program of China (863 Program, No. 2014AA020603), the Science Foundation of Peking University Cancer Hospital (2017-23, 2020-6).

AUTHORS' CONTRIBUTIONS

TG and YHB performed the experiments; SQJ and XFX summarized the data and performed the statistical analyses; XJC, HBH, YH, and HD performed cell experiments, reviewed and edited the manuscript. JFJ designed the project and revised the manuscript. All authors read and approved the final manuscript.

ORCID

Ting Guo  <https://orcid.org/0000-0003-0199-5639>

Yan-Hua Bai  <https://orcid.org/0000-0002-7634-282X>

Xiao-Jing Cheng  <https://orcid.org/0000-0002-5467-791X>
 Hai-Bo Han  <https://orcid.org/0000-0003-2240-5546>
 Hong Du  <https://orcid.org/0000-0002-1107-2902>
 Ying Hu  <https://orcid.org/0000-0002-6330-8032>
 Shu-Qin Jia  <https://orcid.org/0000-0001-6688-0408>
 Xiao-Fang Xing  <https://orcid.org/0000-0002-5707-3396>
 Jia-Fu Ji  <https://orcid.org/0000-0001-6878-5543>

REFERENCES

- Torre LA, Bray F, Siegel RL, Ferlay J, Lortet-Tieulent J, Jemal A. Global cancer statistics, 2012. *CA Cancer J Clin.* 2015;65(2):87–108.
- Chen W, Zheng R, Baade PD, Zhang S, Zeng H, Bray F, et al. Cancer statistics in china, 2015. *CA Cancer J Clin.* 2016;66(2):115–132.
- Massarrat S, & Stolte M. Development of gastric cancer and its prevention. *Arch Iran Med.* 2014;17(7):514–520.
- Kim J-H, Jang Y-J, Park S-S, Park S-H, Kim S-J, Mok Y-J, et al. Surgical outcomes and prognostic factors for t4 gastric cancers. *Asian J Surg.* 2009;32(4):198–204.
- Karlsson O, Thor S, Norberg T, Ohlsson H, Edlund T. Insulin gene enhancer binding protein isl-1 is a member of a novel class of proteins containing both a homeo- and a cys-his domain. *Nature.* 1990;344(6269):879–882.
- Du A, Hunter CS, Murray J, Noble D, Cai C-L, Evans SM, et al. Islet-1 is required for the maturation, proliferation, and survival of the endocrine pancreas. *Diabetes.* 2009;58(9):2059–2069.
- Zhang H, Wang W-P, Guo T, Yang Ji-C, Chen P, Ma K-T, et al. The lim-homeodomain protein isl1 activates insulin gene promoter directly through synergy with beta2. *J Mol Biol.* 2009;392(3):566–577.
- Wang W, Shi Q, Guo T, Yang Z, Jia Z, Chen P, et al. Pdx1 and isl1 differentially coordinate with epigenetic modifications to regulate insulin gene expression in varied glucose concentrations. *Mol Cell Endocrinol.* 2016;428:38–48.
- Jonsson J, Carlsson L, Edlund T, Edlund H. Insulin-promoter-factor 1 is required for pancreas development in mice. *Nature.* 1994;371(6498):606–609.
- Liang X, Song MR, Xu Z, Lanuza GM, Liu Y, Zhuang T, et al. Isl1 is required for multiple aspects of motor neuron development. *Mol Cell Neurosci.* 2011;47(3):215–222.
- Liu Y, Li Y, Li T, Lu H, Jia Z, Wang W, et al. Pou homeodomain protein oct1 modulates islet 1 expression during cardiac differentiation of p19cl6 cells. *Cell Mol Life Sci.* 2011;68(11):1969–1982.
- Zhang Q, Yang Z, Jia Z, Liu C, Guo C, Lu H, et al. Isl-1 is over-expressed in non-hodgkin lymphoma and promotes lymphoma cell proliferation by forming a p-stat3/p-c-jun/isl-1 complex. *Mol Cancer.* 2014;13:181.
- Guo T, Wen X-Z, Li Z-Y, Han H-B, Zhang C-G, Bai Y-H, et al. Isl1 predicts poor outcomes for patients with gastric cancer and drives tumor progression through binding to the zeb1 promoter together with setd7. *Cell Death Dis.* 2019;10(2):33.
- Shi Q, Wang W, Jia Z, Chen P, Ma K, Zhou C. Isl1, a novel regulator of ccnb1, ccnb2 and c-myc genes, promotes gastric cancer cell proliferation and tumor growth. *Oncotarget.* 2016;7(24):36489–36500.
- Agaimy A, Erlenbach-Wünsch K, Konukiewitz B, Schmitt AM, Rieker RJ, Vieth M et al. Isl1 expression is not restricted to pancreatic well-differentiated neuroendocrine neoplasms, but is also commonly found in well and poorly differentiated neuroendocrine neoplasms of extrapancreatic origin. *Mod Pathol.* 2013;26(7):995–1003.
- Schmitt AM, Riniker F, Anlauf M, Schmid S, Soltermann A, Moch H, et al. Islet 1 (isl1) expression is a reliable marker for pancreatic endocrine tumors and their metastases. *Am J Surg Pathol.* 2008;32(3):420–425.
- Liberti MV, Locasale JW. The warburg effect: How does it benefit cancer cells? *Trends Biochem Sci.* 2016;41(3):211–218.
- Gatenby RA, Gillies RJ. Why do cancers have high aerobic glycolysis? *Nat Rev Cancer.* 2004;4(11):891–899.
- Warburg O. On the origin of cancer cells. *Science.* 1956;123(3191):309–314.
- Warburg O. On respiratory impairment in cancer cells. *Science.* 1956;124(3215):269–270.
- Diaz-Ruiz R, Rigoulet M, Devin A. The warburg and crabtree effects: on the origin of cancer cell energy metabolism and of yeast glucose repression. *Biochim Biophys Acta.* 2011;1807(6):568–576.
- Hanahan D, Weinberg RA. Hallmarks of cancer: the next generation. *Cell.* 2011;144(5):646–674.
- Macheda ML, Rogers S, Best JD. Molecular and cellular regulation of glucose transporter (glut) proteins in cancer. *J Cell Physiol.* 2005;202(3):654–662.
- Calvo MB, Figueroa A, Pulido EG, Campelo RG, Aparicio LA. Potential role of sugar transporters in cancer and their relationship with anticancer therapy. *Int J Endocrinol.* 2010;2010.
- Mishra RK, Wei C, Hresko RC, Bajpai R, Heitmeier M, Matulis SM, et al. In silico modeling-based identification of glucose transporter 4 (glut4)-selective inhibitors for cancer therapy. *J Biol Chem.* 2015;290(23):14441–14453.
- Zhao Y, Butler EB, Tan M. Targeting cellular metabolism to improve cancer therapeutics. *Cell Death Dis.* 2013;4:e532.
- Pezzuoto A, D'ascanio M, Ricci A, Pagliuca A, Carico E. Expression and role of p16 and glut1 in malignant diseases and lung cancer: A review. *Thorac Cancer.* 2020;11(11):3060–3070.
- Kocdor MA, Kocdor H, Pereira JS, Vanegas JE, Russo IH, Russo J. Progressive increase of glucose transporter-3 (glut-3) expression in estrogen-induced breast carcinogenesis. *Clin Transl Oncol.* 2013;15(1):55–64.
- Rudlowski C, Becker AJ, Schroder W, Rath W, Büttner R, Moser M. Glut1 messenger rna and protein induction relates to the malignant transformation of cervical cancer. *Am J Clin Pathol.* 2003;120(5):691–698.
- Mao A, Zhou X, Liu Y, Ding J, Miao A, Pan G. Klf8 is associated with poor prognosis and regulates glycolysis by targeting glut4 in gastric cancer. *J Cell Mol Med.* 2019;23(8):5087–5097.
- Zorzano A, Wilkinson W, Kotliar N, Thoidis G, Wadzinski BE, Ruoho AE, et al. Insulin-regulated glucose uptake in rat adipocytes is mediated by two transporter isoforms present in at least two vesicle populations. *J Biol Chem.* 1989;264(21):12358–12363.
- Wang ZM, Cui YH, Li W, Chen S-Y, Liu T-S. Lentiviral-mediated sirna targeted against osteopontin suppresses the growth and metastasis of gastric cancer cells. *Oncol Rep.* 2011;25(4):997–1003.
- Simitsidellis I, Esnal-Zuffiaure A, Kelepouri O, O'flaherty E, Gibson DA, Saunders PTK. Selective androgen receptor

- modulators (sarms) have specific impacts on the mouse uterus. *J Endocrinol.* 2019;242(3):227–239.
34. Grabner B, Schramek D, Mueller KM, Moll HP, Svinka J, Hoffmann T, et al. Disruption of stat3 signalling promotes kras-induced lung tumorigenesis. *Nat Commun.* 2015;6:6285.
 35. Crowley LC, Marfell BJ, Waterhouse NJ. Analyzing cell death by nuclear staining with hoechst 33342. *Cold Spring Harb Protoc.* 2016;2016(9).
 36. Yang Z, Zhang Q, Lu Q, Jia Z, Chen P, Ma K, et al. Isl-1 promotes pancreatic islet cell proliferation by forming an isl-1/set7/9/pdx-1 complex. *Cell Cycle.* 2015;14(24):3820–3829.
 37. Kanehisa M, Furumichi M, Tanabe M, Sato Y, Morishima K. Kegg: new perspectives on genomes, pathways, diseases and drugs. *Nucleic Acids Res.* 2017;45(D1):D353–D361.
 38. Subramanian A, Kuehn H, Gould J, Tamayo P, Mesirov JP. Gseap: a desktop application for gene set enrichment analysis. *Bioinformatics.* 2007;23(23):3251–3253.
 39. Jia B, Zhao X, Wang Y, Wang J, Wang Y, Yang Y. Prognostic roles of mage family members in breast cancer based on km-plotter data. *Oncol Lett.* 2019;18(4):3501–3516.
 40. Tang Z, Li C, Kang B, Gao G, Li C, Zhang Z. Gepia: a web server for cancer and normal gene expression profiling and interactive analyses. *Nucleic Acids Res.* 2017;45(W1):W98–W102.
 41. Camp RL, Dolled-Filhart M, Rimm DL. X-tile: a new bioinformatics tool for biomarker assessment and outcome-based cut-point optimization. *Clin Cancer Res.* 2004;10(21):7252–7259.
 42. Chen L, Cheng X, Tu W, Qi Z, Li H, Liu F, et al. Apatinib inhibits glycolysis by suppressing the vegfr2/akt1/sox5/glut4 signaling pathway in ovarian cancer cells. *Cell Oncol (Dordr).* 2019;42(5):679–690.
 43. Arredouani A, Diane A, Khattab N, Bensmail I, Aoude I, Chikri M, et al. Dnajb3 attenuates metabolic stress and promotes glucose uptake by eliciting glut4 translocation. *Sci Rep.* 2019;9(1):4772.
 44. Mathupala SP, Rempel A, Pedersen PL. Glucose catabolism in cancer cells: identification and characterization of a marked activation response of the type II hexokinase gene to hypoxic conditions. *J Biol Chem.* 2001;276(46):43407–43412.
 45. Semenza GL. Hif-1 mediates metabolic responses to intratumoral hypoxia and oncogenic mutations. *J Clin Invest.* 2013;123(9):3664–3671.
 46. Yun J, Rago C, Cheong I, Pagliarini R, Angenendt P, Rajagopalan H, et al. Glucose deprivation contributes to the development of kras pathway mutations in tumor cells. *Science.* 2009;325(5947):1555–1559.
 47. Miller DM, Thomas SD, Islam A, Muench D, Sedoris K. C-myc and cancer metabolism. *Clin Cancer Res.* 2012;18(20):5546–5553.
 48. Hay N. Reprogramming glucose metabolism in cancer: can it be exploited for cancer therapy? *Nat Rev Cancer.* 2016;16(10):635–649.
 49. Guo T, Wang W, Zhang H, Liu Y, Chen P, Ma K, et al. Isl1 promotes pancreatic islet cell proliferation. *PLoS One.* 2011;6(8):e22387.
 50. Schwartzberg-Bar-Yoseph F, Armoni M, Karnieli E. The tumor suppressor p53 down-regulates glucose transporters glut1 and glut4 gene expression. *Cancer Res.* 2004;64(7):2627–2633.
 51. Chan DA, Sutphin PD, Nguyen P, Turcotte S, Lai EW, Banh A, et al. Targeting glut1 and the warburg effect in renal cell carcinoma by chemical synthetic lethality. *Sci Transl Med.* 2011;3(94):94ra70.
 52. Wang Q, Chen C, Ding Q, Zhao Y, Wang Z, Chen J, et al. Mettl3-mediated m(6)a modification of hdgf mRNA promotes gastric cancer progression and has prognostic significance. *Gut.* 2020;69(7):1193–1205.
 53. Gao R, Liang X, Cheedipudi S, Cordero J, Jiang X, Zhang Q, et al. Pioneering function of isl1 in the epigenetic control of cardiomyocyte cell fate. *Cell Res.* 2019;29(6):486–501.
 54. Wang Y, Li Y, Guo C, Lu Q, Wang W, Jia Z, et al. Isl1 and jmjd3 synergistically control cardiac differentiation of embryonic stem cells. *Nucleic Acids Res.* 2016;44(14):6741–6755.
 55. Radford EJ. Exploring the extent and scope of epigenetic inheritance. *Nat Rev Endocrinol.* 2018;14(6):345–355.

SUPPORTING INFORMATION

Additional supporting information may be found online in the Supporting Information section at the end of the article.

How to cite this article: Guo T, Bai Y-H, Cheng X-J, et al. Insulin gene enhancer protein 1 mediates glycolysis and tumorigenesis of gastric cancer through regulating glucose transporter 4. *Cancer Commun.* 2021;41:258–272.

<https://doi.org/10.1002/cac2.12141>